

A mechanistic model explaining ligand affinity for, and partial agonism of, cannabinoid receptor 1

Fred Shahbazi^{†*}, Daniel Meister^{†*}, Sanam Mohammadzadeh, John F. Trant^{*},

*Department of Chemistry and Biochemistry, University of Windsor, 401 Sunset Avenue,
Windsor ON, N9B 3P4, Canada*

[†] These authors contributed equally to the work.

^{*} Corresponding authors' email: farsheed@uwindsor.ca, j.trant@uwindsor.ca,
meister@uwindsor.ca,

ABSTRACT

CB1, a member of the G protein-coupled receptor class, is the putative protein target of THC, the psychoactive component of cannabis. To better identify new synthetic cannabinoids with increased activity, all cannabinoids with reported experimental binding to the CB1 receptor were modelled *in silico* to build a predictive model for CB1 affinity of small molecules. Computationally derived affinity is not sufficient in and of itself to predict binding, but coupled with the experimental evidence that ligands enter the receptor from the membrane rather than solvent, we provide a model that accurately describes the binding of these molecules by incorporating a correction factor for relative hydrophobicity. In addition, we propose a mechanism of action for partial CB1 agonists based on molecular dynamics simulations of **THC** homologues, modelling long time scale structural changes in the CB1 receptor. Together, the affinity model, and the mechanism of agonism/antagonism can allow for the computational prediction of both the effective behaviour and potency of novel cannabinoids, and several such predictions are made.

Keywords: Cannabis, molecular modeling, THC, partial agonist, GPCR, cannabinoid receptor 1, CB1

Introduction

Cannabinoids, a family of alkyl resorcinol-functionalized diterpenes produced by *C. sativa*, act primarily through agonism and antagonism of human G-protein-coupled receptors (GPCRs).¹ Tetrahydrocannabinol (**THC**) is a well-established partial agonist of cannabinoid receptor 1 (CB1) where it occupies the orthosteric site, the binding site for endogenous ligands. Full agonists open up the G-protein binding domain on the cytosolic side of the protein, while antagonists prevent G-protein binding by inducing a conformational change that closes the site. Partial agonists have intermediate activity. The majority of drugs that target GPCRs act at the orthosteric site.² Since the initial discovery of **THC** and other related cannabinoids, numerous modifications and analogs have been synthesized in an attempt to define the structure–activity relationship (SAR) of **THC** with both CB1 and CB2. **THC** analogues differ primarily at two major sites: the ring system and the alkyl chain (Fig 1A). According to Bow and co-workers, the length of the alkyl chain is the key parameter for determining CB1 receptor activity; a minimum of three carbons is necessary to bind the receptor, with activity peaking at eight-carbons and falling off as length increases past that point (Fig 1B).³

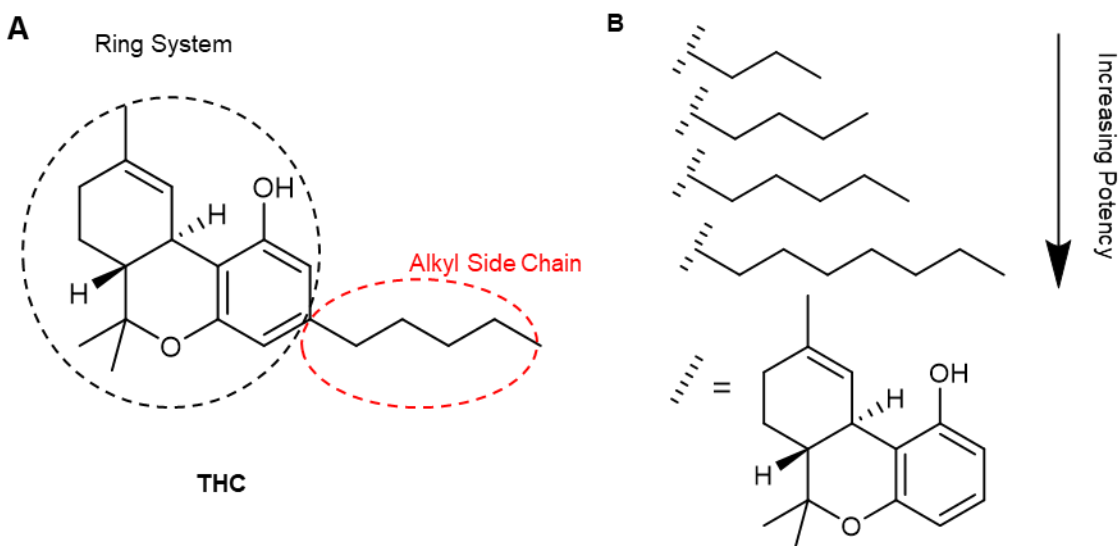


Figure 1. Overview of **THC** and its ring system, highlighting the various side chain lengths discussed in the article.

Recently, Citti et al isolated novel phytocannabinoids Tetrahydrocannabiphorol (**THCP**),⁴ with a seven-carbon alkyl chain, and tetrahydrocannabutol (**THCB**)⁵ with a four-carbon

alkyl chain. Both had higher *in vitro* binding activity (K_i = 1.2 and 15 nM, respectively) than that reported for five-carbon **THC** (K_i = 40 nM).^{3, 5} Citti proposes that this differential activity arises because the orthosteric binding site of CB1 has three hydrophobic pockets⁶: The main hydrophobic pocket (**M-pocket**) which houses the ring system of **THC** homologs; the long hydrophobic pocket (**L-pocket**) formed by TMs III, V, and VI, which can accommodate the long heptyl chain of **THCP** and the pentyl chain of **THC**; and the hydrophobic sub-pocket (**S-pocket**) formed by Phe170, Phe200, Leu387, Met363, Leu359, and Cys386 that lies towards the toggle switch residues needed to activate the receptor; this is located at the intersection between the **M-pocket** and the **L-pocket** (**Figure S2 and Video S1**). As they are too short to benefit from the hydrophobic **L-pocket**, the propyl and butyl chains of **THCV** and **THCB** instead sit in the **S-pocket**. Citti argues that this is the reason for **THCB**'s higher affinity for CB1 than the longer **THC**.⁴⁻⁵ However these new findings contradict the literature: first, **THC** analogues with alkyl chains shorter than 5 or longer than 8 methylenes have decreased binding affinity compared to those in the middle, with affinity peaking at 8 carbons as noted.³ However, they report that four-carbon **THCB** (K_i = 15 nM) has higher binding affinity than five-carbon **THC** (K_i = 40 nM). Second, the binding affinity of **THCP** and **THCB** were compared to the **THC** and **THCV** affinity values reported by Bow and Rimoldi.³ Several binding affinities have been reported for **THC** (K_i = 40³, 35.64⁷, 25.1⁸, 5.05⁹ and 2.9¹⁰) and **THCV** (K_i = 75.4³, 46.6¹¹ and 22¹²). There is a large variation in the experimental data available in the literature, this implies that careful remeasurement of these values is in order, and great caution must be taken in overreliance and overinterpretation of small differences. Finally, interaction of a ligand with the centrally located W356^{6,48} and F200^{3,36} toggle switch differentiates whether a given ligand is an agonist, "triggering" the switch and inducing the conformational change on the cytoplasmic side of the protein allowing for G-protein interaction; or an antagonist, occupying the pocket and preventing the switch being triggered.¹

This result intersects with our own interest in this receptor and defining precisely how the ligands interact. We understand the mechanism of action of the agonists, but it is less clear that there is a well understood mechanism of action for partial agonists. What makes them partial? Lacking any crystallographic data with any phytocannabinoid, this

question remains outstanding. Furthermore, it highlights that we have an imprecise understanding of the experimental binding affinity, even for these well studied major cannabinoids, with reasonable estimates of the K_i varying by over an order of magnitude. We wished to develop a theoretical model for determining binding affinity. Generally this is done using an all atom molecular modelling study, but this provided inconsistent results: affinity for the receptor was not sufficient, in and of itself, to describe the observed K_i . This however can partially be explained by the different mode of entry of ligands into CB1 compared to many G-protein-coupled receptors: it enters from the lipid membrane, not the solvent. With this information, and using a library of 21 **THC** homologues with experimental data (Figure 2), we propose a mathematical model to predict the affinity of a ligand for CB1, and a conceptual model to determine whether a ligand is likely to be agonist, antagonist, or partial agonist, and propose a mechanism by which partial agonists function as such. During the preparation of this article, Shukla and colleagues published on the mechanism of action of THC as a partial agonist using complementary techniques to our own, providing further confidence in the reliability of our conclusion.¹³

Results and Discussion

To predict the binding affinity between ligands and receptors as well as to characterize the different binding modes an *in silico* study was conducted on a total of 21 **THC** homologues with experimentally measured binding affinity, including the antagonist **THC**,⁶ weak agonists **THCA**,¹⁴ partial agonists **THCB** and **THC**,⁵ and agonists **THCP**, **AM11542**, **AM841**, **AM12033**, **AM4030**, **HU-210**, ajulemic acid (**AJA**) and **Nabilone** of CB1 which have various activities and selectivity (Figure 1).

We investigated several parameters to attempt to develop a model providing a reliable and accurate correlation between experimental binding affinity and *in silico* docking results. First, we examined rigid-receptor docking (RRD) with scaled van der Waals radii of non-polar atoms (1.0, 0.8, and 0.6) to represent some of the flexibility present within the receptor, an approach well preceded to provide good correlation to experiment.¹⁵ It generally works best when the initial protein structure best reflects the binding mode of the specific class of ligands, a reasonable expectation seeing the superficial similarity of the ligand library. The docking was followed by further analysis to better determine the free energy of the complex (and consequently the binding energy)

using MM-GBSA calculations.¹⁶ These analyses began with the lowest energy docked conformer in each case, once this pose was visually confirmed to be a reasonable conformer. The experimental *k_i* values, rigid docking scores (RRD) and MM-GBSA predicted binding free energies are listed in Table 1.

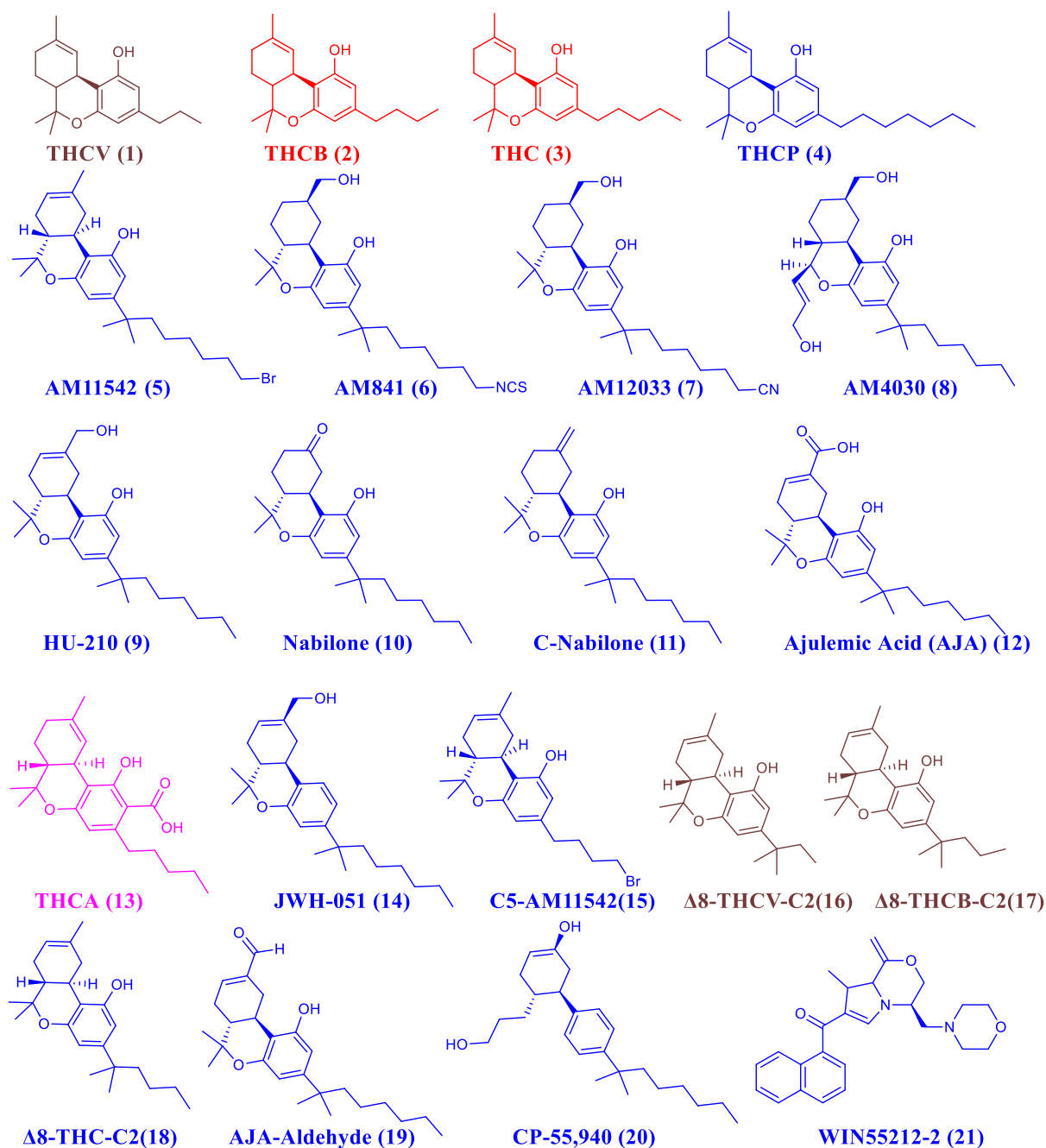


Figure 2. Structures of the **THC** analogues with known experimental binding affinities used in this study. Those in red are partial agonists, in pink weak agonists, in blue potent agonists, in brown antagonists.

Table 1. RRD scores and predicted binding-free energies (kcal/mol) obtained by Prime/MM–GBSA of the CB1 ligands									
Ligand	K_i (nM) ^a	r_w scaling factor Rigid Docking Score (Kcal/mol)			MM–GBSA ΔG_{bind} (kcal/mol)			Induced Docking Score (Kcal/mol)	LogP
		1.0	0.8	0.6	1.0	0.8	0.6		
THCV (1)	22 ¹²	-9.12	-8.63	-7.99	-62.09	-54.83	-51.64	-10.81	4.91
THCB (2)	15 ⁵	-9.92	-8.99	-8.24	-62.78	-56.16	-54.25	-10.98	5.30
THC (3)	2.9 ^{10, 17}	-10.13	-9.07	-8.52	-61.93	-63.9	-55.76	-11.51	5.66
THCP (4)	1.2 ⁴	-5.07	-8.65	-8.02	-57.09	-55.65	-67.06	-11.81	6.44
AM11542 (5)	0.11 ¹⁸	-8.51	-8.70	-8.05	-55.01	-68.11	-67.90	-12.65	7.58
AM841 (6)	1.14 ¹⁹	-3.03	-11.36	-8.89	-47.70	-77.74	-73.36	-11.73	5.98
AM12033 (7)	0.51 ¹⁹	-9.34	-10.03	-9.47	-70.63	-70.08	-73.55	-13.46	4.30
AM4030 (8)	0.7 ²⁰	-5.44	-8.68	-9.07	-49.09	-64.51	-62.58	-12.28	5.34
HU-210	0.73 ²¹	-8.68	-9.425	-8.25	-81.01	-68.02	-76.49	-12.18	5.83
Nabilone (10)	2.19 ²²	-9.75	-8.53	-7.78	-70.71	-69.33	-68.00	-11.91	5.50
C-Nabilone (11)	1.82 ²²	-5.45	-8.97	-7.51	-64.13	-58.11	-37.19	-11.60	6.72
AJA (12)	32.2 ²³	---	-9.45	-7.61	---	-55.43	-43.35	-10.62	5.83
THCA (13)	23.51 ⁷	---	-5.98	-5.07	---	-34.99	-34.16	-10.89	5.59
JWH-051 (14)	1.2 ²⁴	-9.25	-8.61	-6.92	-68.3	-71.1	-71.67	-12.10	6.56
C5-AM11542 (15)	10.8 ²⁵	-9.88	-9.59	-7.85	-61.45	-65.45	-66.44	-10.88	5.90
Δ^8 -THCV-C2 (16)	14 ²⁶	-8.87	-9.27	-7.9	-62.07	-59.49	-61.29	-10.50	5.99
Δ^8 -THCB-C2 (17)	10.9 ²⁶	-8.48	-8.79	-8.15	-66.37	-55.06	-65.55	-10.74	5.59
Δ^8 -THC-C2 (18)	3.9 ²⁶	-8.51	-8.83	-7.80	-63.39	-64.84	-50.54	-11.27	5.79
AJAldehyde (19)	2.24 ²²	-7.39	-9.27	-8.03	-64.5	-68.4	-64.81	-12.03	5.70
CP55940 (20)	0.58 ²¹	-9.45	-8.71	-7.31	-67.49	-58.55	-74.27	-12.35	5.10
Win55212-2 (21)	1.9 ²⁷	---	---	-6.25	---	---	-49.21	-12.35	4.15

^a For ligands where multiple K_i values have been reported in the literature, the lowest reported value was selected; with the differences in reported values ranging to an order of magnitude and dependent on the tool used to measure the value, there is error built into our model. The lone exception is for **HU-210**, where the employed reported value of 0.73 nM is higher than the lowest value, 0.25 nM. This provides better correlation with our model, suggesting that the higher value may prove more correct should the value be redetermined by a third measurement.

^b --- indicates that the ligand does not dock to the orthosteric binding site of CB1.

There is only weak correlation between the experimental values ($\log K_i$ (nM)) and the RRD score (kcal/mol; Fig 3A, Fig S1). The Pearson correlation coefficient (R^2) is 0.081, 0.065, and 0.110 for r_w scaling factors 1.0, 0.8 and 0.6, respectively. This is an extremely poor correlation. An MM-GBSA refinement does little to improve the correlations, and although it does become statistically significant with r_w scaling factors of 0.8 or 0.6, this remains a

poor tool for predicting binding affinity. This suggests that there might be more adjustments occurring in the receptor depending on very fine details of the ligand than one would necessarily expect based on their similarity by inspection. This both implies that induced docking might prove more useful, and that mechanism might be dependent on minor adjustments to the binding pocket.

Induced fit docking (IFD), a computationally far more expensive approach than RRD, allows for considerable flexibility in the binding site residues which works well for systems with moderate flexibility and differences in the binding mode of various ligands.²⁸ This can be important if the initial pocket in a given conformation is too restrictive or permissive to accommodate a ligand (meaning the RRD will be artificially poor), and both the pocket and ligand must mutually adapt to each other when forming a complex.²⁹ However, IFD can introduce additional errors in measurement if the pocket is too flexible, and can be less useful for prediction than RRD if the ligand classes are all similar to one another. IFD generally shows better results in reproducing the native conformations of complexes,³⁰ and this was used with all 21 ligands (Table 2).

Even on a simple perusal, these results seem to reflect what we know from experimental science: increasing the number of side chain carbon atoms in the series from **THCV** to **THCP** leads to improved docking scores. Overall, the correlation between the experimental values ($\log k_i(\text{nM})$) and IFD (kcal/mol) has dramatically improved compared to RRD. The Pearson correlation coefficient (R^2) is 0.807 with a $p\text{-value} < 1 \times 10^{-5}$ (Fig 3C). However, there are several ligands whose behaviour is not consistent with the model, such as **AM12033** and **AM11542**. This could be simply that no model is perfect, and that we should be satisfied with a good correlation, or, it could be that free energy of binding alone does not model the system correctly.

Let us consider the assumptions of the system. Efficacy depends on several factors beyond simply the affinity of a drug for its target, including the ability of the drug to enter the cell, the stability of the drug over the lifetime of the experiment, and whether it is sequestered through some competing biochemical mechanism. All of these essentially affect the localized concentration of the drug. Generally, for drugs with a similar scaffold, many of these features would be expected to be largely equivalent. Furthermore, most GPCRs, indeed most membrane proteins, interact with their ligand in

the bulk extracellular fluid, so many of these mechanisms are not relevant. However, Class A GPCRs can have their orthosteric site opening into the lipid bilayer, and CB1 is one such protein.¹ Consequently, the relevant concentration is not the concentration of the drug in solution, but rather the concentration of the drug in the lipid bilayer and these are not the same. Consider two drugs with the same binding affinity for a type A GPCR like CB1 that differ only in their water solubility: hydrophobic **A**, and hydrophilic **B**. For the same bulk concentration, **A** would be expected to partition into the lipid bilayer to a greater degree than **B**. This would give **A** a higher localized concentration to bind with the GPCR. Cannabinoids enter the cannabinoid receptors via the lipid bilayer.³¹ Recently, Hurst and *at el.* demonstrated *via* molecular dynamics that ligands access the binding pockets of other class A GPCRs *via* the lipid bilayer.³² This is consistent with our models where during all MD simulations, the orthosteric site's opening never left the lipid bilayer.

Lipophilicity can be expressed as the logarithm of the partition coefficient (logP) between 1-octanol and water.³³ The prediction of this parameter is a key tool in modern drug design.³⁴ We utilized the log(P) for all 21 ligands, obtained using QikProp (Table 1).³⁵ We then used the imperialist competitive algorithm (ICA), as implemented in MATLAB,³⁶ to generate a series of best fit equations to the data set with different exponential forms, constants, and relationships between the binding term, derived from the IFD binding, and the hydrophobicity partition term, derived from log(P).³⁷ The best fit equation improved the Pearson correlation coefficient square (R^2) from 0.81 to 0.92 (Fig 3D), and correctly shifted the “outlier” ligands towards the trend; partition ability into the lipid bilayer explains the discrepancy between **AM12033** and **AM11542** binding affinity and efficacy. The equation of our fit is as follows:

Optimized Fit:
$$Ki = (X + 13.166)/1.1755$$

Where Ki is measured in nM and $X = IFD\ Score - 0.03(\log P)^2$. The values of the constants are, of course, empirically derived. To the best of our knowledge, this is the first theoretical framework for predicting efficacy based on combining binding affinity calculated through all-atomistic modelling, and hydrophobicity, not only for the cannabinoids but for any class of ligand; we see no reason why this same methodology

could not be applied to any other system where ligands need to partition into compartments, although permeability functions might prove a more useful parameter if the ligand simply needs to passively pass through a bilayer rather than act from the bilayer as in this case.

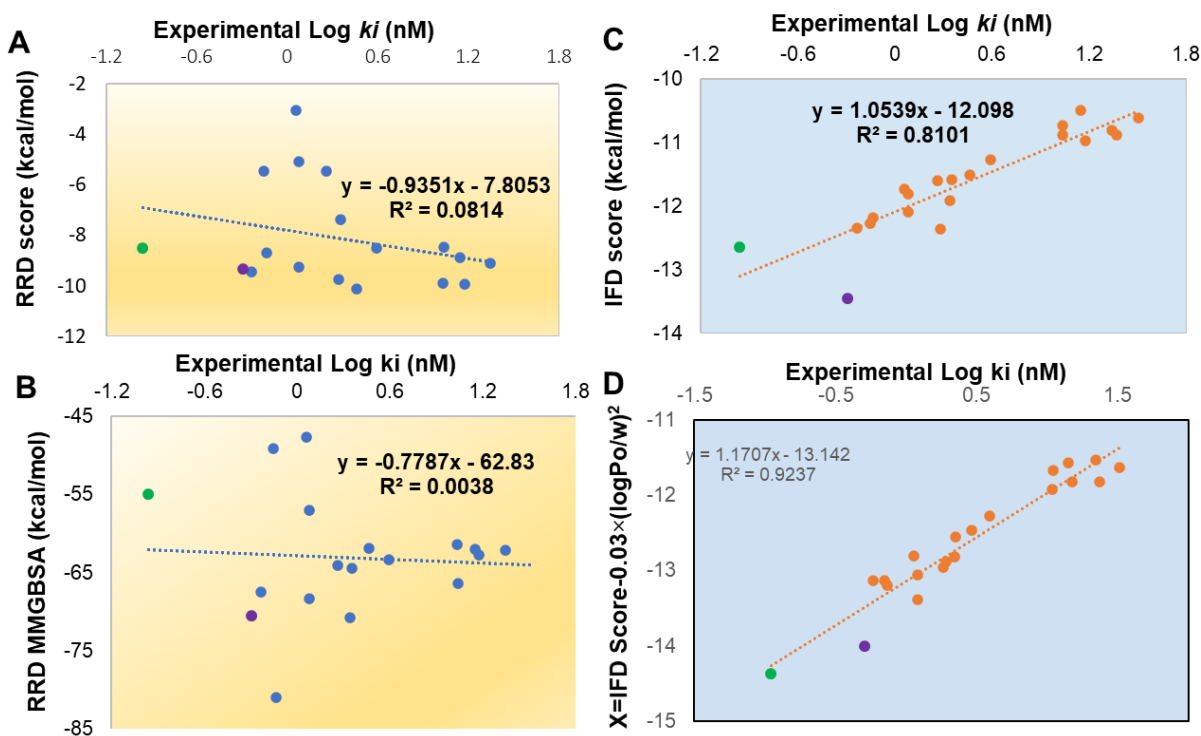


Figure 3. Correlation analysis between experimental values, (A) RRD, (B)MM-GBSA and (C) IFD scores and (D) IFD scores optimized with Lipophilicity. **AM11542** and **AM12033** are shown in Green and Purple colors, respectively.

We then looked at how well the model worked to predict the binding affinities of different analogues. We compared the binding of **Δ^8 -THC**, whose binding affinity for CB1 has been variously reported as 44 nM^{3, 38} or 47 nM with binding predicted by our model.³⁹ The experimental values are far more precise than those provided for many of the other cannabinoids, allowing us to determine whether they are accurate. **Δ^8 -THC** differs from **THC** only by the location of the olefin in Ring C meaning we can expect similar lipophilicity and likely a similar binding mode; under this understanding the values do seem rather high compared to that of **THC** (2.9 nM). Docking the ligand using IFD provides a reasonable conformation, and a calculation of the lipophilicity and its use in our equation

estimates a K_i of 11.02 nM (Table S4) (Fig 4C and 4D). This is lower than **THC** but is likely a more accurate value than those reported in the literature. This is important as one of the reports for **Δ^8 -THC** also estimated the binding affinity of THC to be 40 nM,³ which is an outlier compared to other measurements. Based on our model, we propose that the binding affinity of **Δ^8 -THC** has been significantly underestimated in reports to date, and its value might benefit from re-measurement.

Using our model and our understanding of the structural features responsible for CB1 binding, we prophesize two new related molecules of which we predict one will prove a very high affinity binder and CB1 full agonist, while the other will be inactive. **THC** has been the subject of many structure activity relationship studies (Fig. 4A). Gómez-Jeria and coworkers developed a pharmacophore model for classical cannabinoid-CB1 interactions (Fig. 4B).⁴⁰ The C1 phenol group is required for good selectivity for CB1 over CB2, and we have already extensively discussed the importance of the alkyl chain. Binding affinity can also be enhanced by hydroxylation of the C11 methyl group as can be seen in the AM-series (Fig. 4A).³⁹ Using this information, and aiming for synthetic simplicity, we propose two unknown compounds, both simple **Δ^8 -THC** homologues, **THCN** with 9 methyl groups and **THCU** with 11 methyl groups. We conducted the IFD and calculated the lipophilicity and then predicted the binding affinity based on our model (Fig 4C). The alkyl side chain of **THCN** extends perfectly into **S-pocket** while **THCU** is too long and does not fit into the orthosteric site; it will not be able to fit in the receptor, and we expect it to be largely inactive. The predicted binding constant for **THCN**, is 0.84 nM, which would make it the best binding phytocannabinoid-like molecule. The synthesis of these new compounds is currently underway for their evaluation.

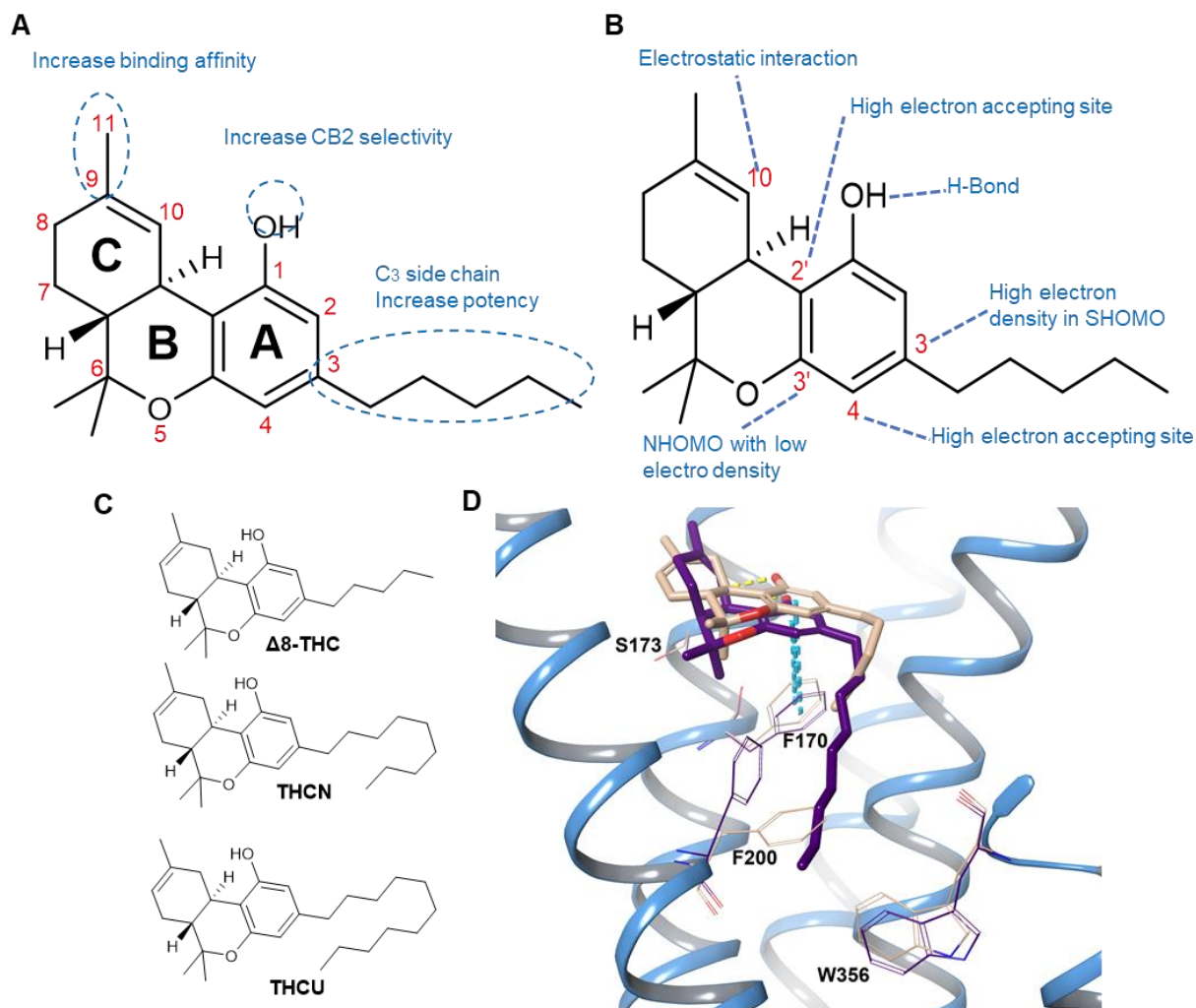


Figure 4. (A) common chemical modifications on **THC** skeleton and (B) Proposed pharmacophore for classical cannabinoids interacting with CB1 receptors. (C) structures of Δ^8 -THC, **THCN** and **THCU**. (D) binding poses of **THCA** (bisque) and **THCN** (indigo) in complex with CB1. In all figures, oxygen is in red, and nitrogen is in blue. H-bonds are represented by yellow dotted lines, and π - π interactions by blue dotted lines. Key residues related to the ligands are highlighted in the same color as their present ligand.

It is important to know which one of reported binding affinities for **THC** and **THCV** is most likely to be accurate. We calculated the correlation of experimental binding affinity and IFD score for all ligands except **THCV** and **THC** (Fig S3). The Pearson correlation coefficient (R^2) was 0.797 or 0.918 for IFD (kcal/mol) and IFD scores optimized with lipophilicity respectively. A calculation of the IFD score and the lipophilicity their

processing through our equation estimates a K_i for **THCV** and **THC** of 26.93 and 4.11 nM respectively, which is near the expected values.

Although determining a model for predicting binding affinity of designer cannabinoids is critical to our current research program, affinity, as can be clearly seen, does not define the functional role of the ligand. Tight binders and weak binders can be either antagonists, partial-agonists, reverse agonists, or full agonists. The specifics are in how the ligand interacts with the receptor.⁶ We have not identified a clear theoretical literature model that differentiates between these roles. Consequently, we more closely investigated the binding mode of the homologous series of **THCV**, **THCB**, **THC** and **THCP** using IFD as differential receptor response to the ligands likely explains why the first is an antagonist, the middle two partial agonists, and the latter a full agonist (Table 2). Highly potent agonist **AM11542** was included as a control.

Table 2. IFD scores and predicted predicted lipophilicity of THC homologues ligands.						
Ligand	IFD Score (kcal/mol)		$\Delta E = E_S - E_L$ (kcal/mol)	Prime/MM-GBSA (kcal/mol)		$\Delta E = E_S - E_L$ (kcal/mol)
	S-pocket Pose	L-pocket Pose		S-pocket Pose	L-pocket Pose	
THCV (1)	-10.37	-10.81	0.44	-66.2	-63.96	2.24
THCB (2)	-10.98	-10.8	-0.18	-65.85	-62.24	-3.61
THC (3)	-11.51	-11.51	-0.07	-58.98	-57.87	-1.11
THCP (4)	-11.81	-10.75	-1.058	-69.61	-67.87	-1.74
AM11542 (5)	-12.65	-10.16	-2.49	-79.26	-74.25	-4.01

THCV, **THCB**, **THC** and **THCP** all adopt similar conformations in the orthosteric ligand-binding site. Their ring systems sit in the M-pocket in nearly superimposable geometries: they only differ in that the alkyl side chains of **THCB**, **THC** and **THCP** protrude into the smaller **S-pocket** towards the receptor-activating toggle switch (formed by F200 and W356), which does not occur for **THCV**, which instead extends into the **L-pocket** (Fig. 5A). The phenolic C1 -OH of all four cannabinoids forms a hydrogen bond with S173; in the case of **THCV** and **THCB**, it forms an additional H-bond with H178 (Fig. S3A). The ring systems, excepting that of **THCV**, participate in π - π interactions with the receptor's F170, which sits at the intersection of the three pockets. Hydrophobic interactions help retain the ligands affinity to the rest of the surface, and, as expected, these interactions increase in strength as the surface area increases due to a lengthening alkyl chain with

the IFD score rising from -10.81 to -11.81 moving through the series from **THCV** to **THCP** (Fig S3).

Interested in mechanism, we focused in on the effects that cannabinoid binding has on the dynamics of the toggle switch formed by F200 and W356, respectively located on transmembrane α -helix 3 (TM3) and TM6. When an alkyl chain pushes between them, it forces open the two helices like chopsticks revealing the Gi-protein binding site on the cytoplasmic face, activating the receptor.⁴¹ Their different positions are best described by comparing their form in the presence of **THC** and the highly potent inverse agonist Taranabant (**TNB**, Fig 5C; PDB ID: 5U09). **TNB@CB1** is akin to the empty inactivated receptor; but reduces its flexibility (hence inverse agonism), locking the two aromatic residues that make up the switch parallel to one another. This holds the transmembrane helices together. The ligand sits in the **M-pocket**, extending its side chain down the **L-pocket** with high affinity to prevent other ligands from binding. **THC** on the other hand, extending its tail into the **S-pocket** pushes the residues open, activating the receptor.

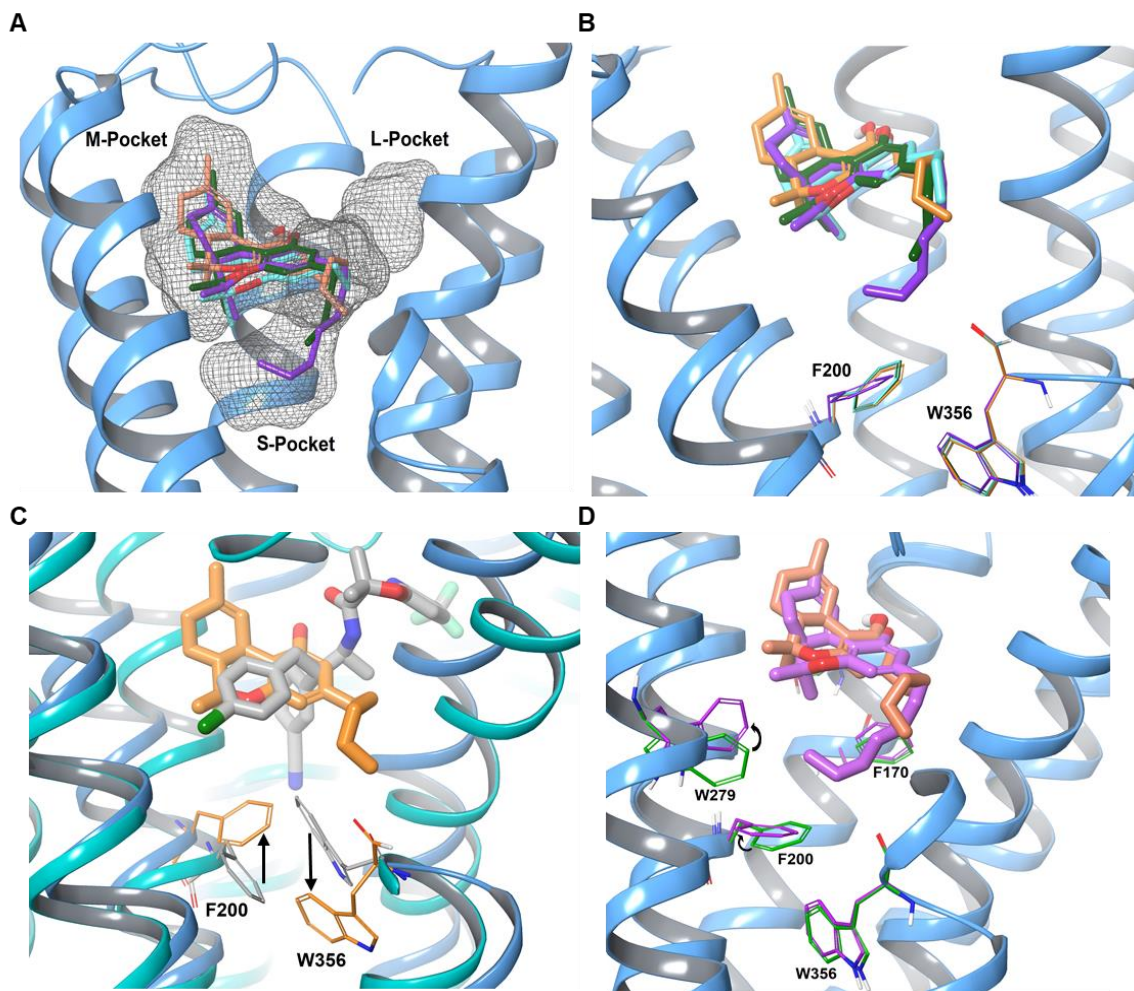


Figure 5. (A) binding poses of **THCV** (Cyan), **THCB** (dark green), **THC** (orange) and **THCP** (purple) in complex with CB1 (PDB ID: 6N4B). (B) binding poses of **THCV**, **THCB**, **THC** in complex with CB1. (C) superimposition of **THC@CB1** and **TNB@CB1** (gray) ligand-binding pockets; (D) binding poses of **THCP** and **THC** in complex with CB1. The oxygen atoms are in red, nitrogen in blue and sulfur in yellow, H-bonds in yellow dotted lines, π - π interactions in blue dotted lines and hydrophobic pocket is bordered in dash dark gray mesh. Key residues related to ligands have the same colors.

THC, along with its shorter homologues **THCV** and **THCB**, all have similar effects on the toggle switch with the key residues adopting the same conformation in the activated form (Figs 5B and 5C). **THCP** extends deeper into this pocket, forcing the residues even further apart, further opening up the G-protein binding site, facilitating activity, and helping to explain its full agonist role (Fig 5D). However, this does not explain

why the shorter analogues are only partial agonists, or why **THCV** is an antagonist, as they interact the same way. The true story is more complicated.

We then turned to the very potent AM-series analogues. Consistent with the literature and published crystal structures,¹ our model places the ring system of all ligands into the **M-pocket**. Most of them extend their alkyl chain into the **S-pocket**, but that of **C5-AM11542** folds back over itself to extend into the **L-pocket** (Fig. S4A). They are all however, highly effective at forcing open the toggle switch, with the distance between F200 and W356 starting higher than for **THC**, and increasing in the order of **C5-AM11452**, **AM4030**, **AM11542**, **AM12033** and **AM841** (Fig. S4A). **AM11542**, **C5-AM11542**, **AM841**, **AM12033** each have one π - π interaction with F170. **AM841**, a covalent inhibitor in its final form, has an extra H-bond with S173 and π - π interaction with F268 when it sits non-covalently in the pocket. The phenolic hydroxyl at C1 of **AM12033** forms a H-bond with H178 and OH group at C11 forms two H-bonds with D176 and S173. **AM4030** forms an extra π - π with F268 and the O-H group of 6 β -((E)-3-hydroxyprop-1-enyl) form H-bond with F268.

Other agonists studied, like **HU-210**, **Nabilone**, **JWH-051**, **Δ^8 -THCV-C2**, **Δ^8 -THCB-C2**, and **Δ^8 -THC-C2** behave very similarly (Fig. S4B). In all cases the **S-pocket**-occupying side chain forces open the toggle switch. Exceptions are **THCA** and **AJA**, which adopt a different conformation in the orthosteric site. The carboxyl group of **THCA** forms two H-bonds, one with S383, the other with H178, which induces a repositioning of the ring system, and consequently the alkyl chain remains in the atrium between the **S**- and **L-pockets** entering neither (Fig. S4C). Unusually, the ring system of **AJA** rotates 180° compared to all other ligands. The carboxyl and phenolic OH- groups form strong H-bonds with K192 and S173, respectively locking this unusual conformation (Fig. S4C). all poses of **C-nabilone** show far different binding, with the ring sitting at the intersection of the **S** and **L pockets** and the alkyl chains sticking up into the **M-pocket** (Fig. S4D). The third lowest energy pose of **AJaldehyde** is identical to the activation state, and its alkyl chain extends to the **S-pocket**. Its docking score is also consistent with the equation, and it marginally improves the R-Squared value when added to the training set (≈ 0.03) (Fig.S4D).

These lowest energy docked conformers, however, fail to capture the complexity of the dynamic binding of the phytocannabinoids. **THC** is a CB1 partial agonist, meaning that upon binding, it does not completely induce the conformational change associated with agonists. There are multiple mechanisms by which this could occur. One would be that in the docked conformation, **THC** simply does not induce enough pressure on the toggle switch to open the G-protein site. This is not supported by our model which predicts that it forces a similar conformation onto the protein as full agonists like **THCP** do. Alternatively, **THC** might drift away from the core of the orthosteric site and occupy a position higher in the cavity as **CBD** is predicted to do in the presence of **THC**. A third possibility is that the alkyl chain can flip from the **S-pocket** to the **L-pocket**. Shao *et al.* computationally docked **THC** to a relaxed receptor derived from the antagonist TNB-bound structure (PDB: 5TGZ).⁴² They predicted that the alkyl side chain of **THC** extends just towards toggle residue W356, and would likely activate it as an agonist. Similarly, when Hua and colleagues docked **THC** to the full-agonist bound structure (PDB: 5XRA),¹⁸ they predicted that **THC** would behave similarly to **AM11542** and that its alkyl side chain of **THC** extend towards F200 and W356. However, in the docking study accompanying their Cryo-EM structure of CB1, Kumar *et al.*⁴³ proposed that **THC**'s alkyl chain is more flexible and potentially able occupy either the **L** or **S-pockets**. This has been further supported by Dutta and colleagues who, like us, proposed that this “switch hitting” behaviour explains the partial agonism of **THC**.¹³ Evidence appears to support that **THCV** and **THCB** protrude into the **S-pocket** towards the toggle switch,⁴⁻⁶ while **THCP** behaves similarly to **THC**, and occupies the **L-pocket**.⁴

As this might help mechanistically explain partial agonism, we analyzed the behavior of the alkyl chains of **THCV**, **THCB**, **THC**, **THCP** and **AM11542** in the orthosteric site. We employed IFD and MM-GBSA refinements of conformations of these ligands occupying both the **S-pocket** and **L-pockets** and calculated the difference in preference for the two pockets ($\Delta E_{S/L}$, Table 2, Fig 6). Among these ligands only **THCV** has a positive $\Delta E_{S/L}$, meaning that it prefers to occupy the non-triggering **L-pocket**. This explains why it is an antagonist. However, the side chain is very short, and does not extend far into either pocket: even when it does insert into the **S-pocket**, it does not disrupt the toggle switch residues (Fig. 6A). **THCV** forms similar hydrophobic interactions in both conformations,

interacting with S383, C382, F379, I362, L359 and F170. For the slightly longer **THCB** and **THC**, the $\Delta E_{S/L}$ are -0.18 and -0.07, respectively. This is essentially 0, meaning that in both cases we would predict that the ligand fluctuates rapidly between occupying the two pockets. Unlike for **THCV**, the toggle switch residues do significantly change orientation depending on the location of the alkyl chain (Fig. 6B). This arises because although both ligands form the same core interactions at the **M-pocket** with C382, F379, I362 and F170 (and, for **THC**, with M363, S383, L359) regardless of the orientation; they differ in their additional interactions when the alkyl chain enters one or the other pocket (Fig. 6C). However, for **THCP** (Fig. 6D) and **AM11542**, $\Delta E_{S/L}$ is high as their alkyl chains are effectively unable to occupy the **L-pocket** if the ring system is in a reasonable position within the **M-pocket**. This means they are locked into a conformation that forces open the toggle switch. They cannot move their alkyl chain into the non-activating **L-pocket**. This means that when bound, they must activate the toggle switch, explaining why they are full agonists.

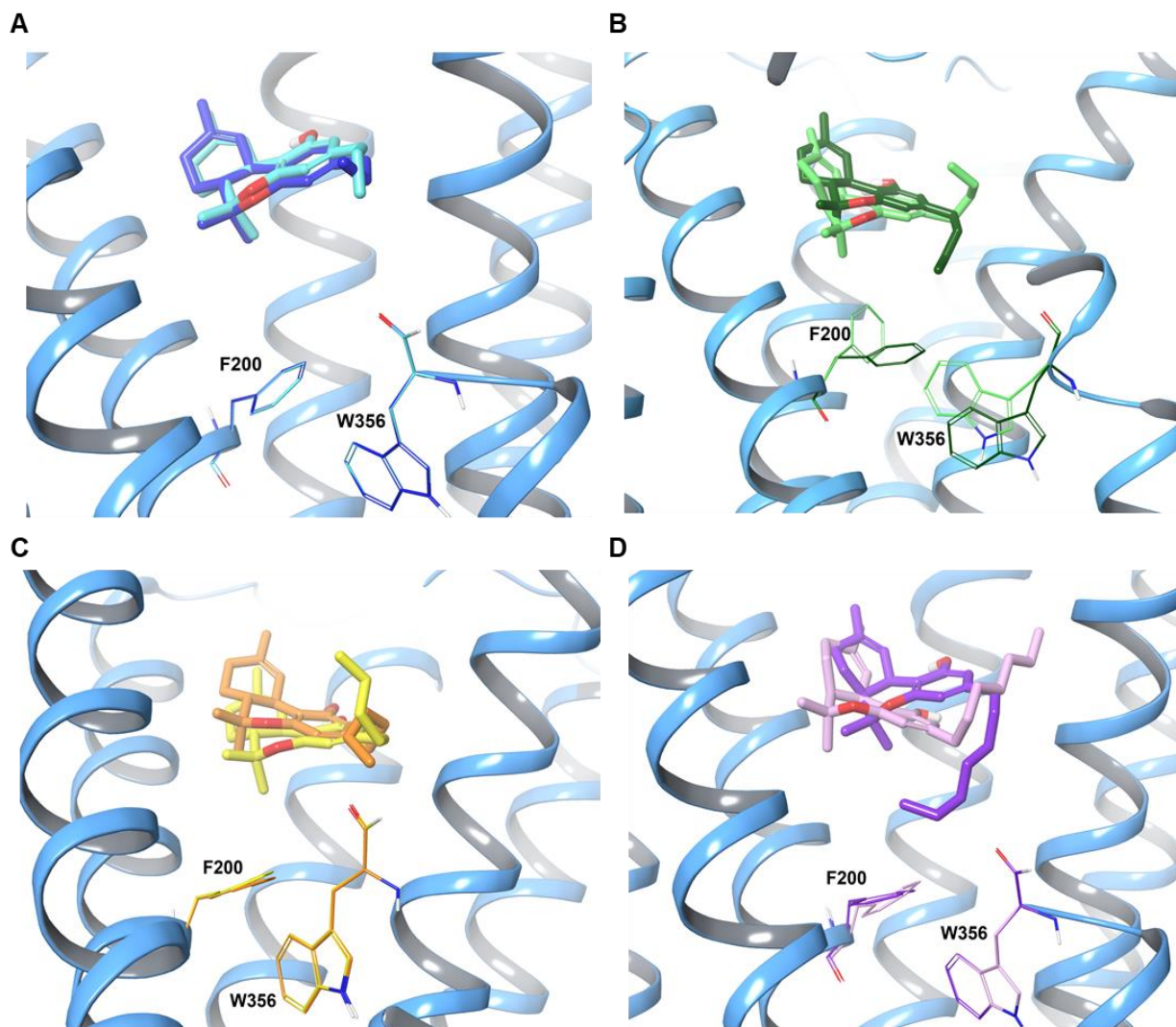


Figure 6. Superimposed docking poses of ligands (A) **THCV** in the **L-pocket** (cyan) and **S-pocket** (blue), (B) **THCB** in the **L-pocket** (dark green) and **S-pocket** (light green), (C) **THC** in the **L-pocket** (yellow) and **S-pocket** (orange), (D) **THCP** in the **L-pocket** (purple) and **S-pocket** (rosepink). Ribbons are shown in light blue color and residues are colored as same as their related ligands.

MD simulations of **THCV**, **THCB**, **THC** and **THCP** and **AM11542** in the **L** or **S pocket** were performed to investigate their effects on CB1 activation via their interaction with toggle residues and conformational changes in the CB1 transmembrane helices. The complexes were embedded in a POPC membrane and solvated, with NaCl ions added to

bring the concentration of the solution to 0.15M. Simulations were then run for 200ns and then analyzed by clustering to obtain the most representative structure at the end of the simulation. CB1 activation is characterized by the outward movement of TM5, TM6 and TM7 after the ligand interacts with toggle residues F200 and W356, which opens the G-protein binding pocket. In the case of **AM11542**, an agonist, clear activation and helix movement is observed when compared to the inactive receptor (Fig. 7A). For **THCV**, very little movement is observed in the helices. This agrees with the experimental observations that it is an antagonist as receptor activation is not observed. In the cases of **THB**, **THC** and **THCP**, some helical movement is observed and a partial opening of the g-protein binding site. The most notable change was observed in **THCP** which showed the largest movement of TM5 and TM6, though changes were not as pronounced as in **AM11542**, as **THCP** had begun migrating out of the binding pocket. In all cases besides **THCV**, the ligands bound with the side chain in the **L-pocket** exhibited greater movement in the helices than those in the **S-pocket**.

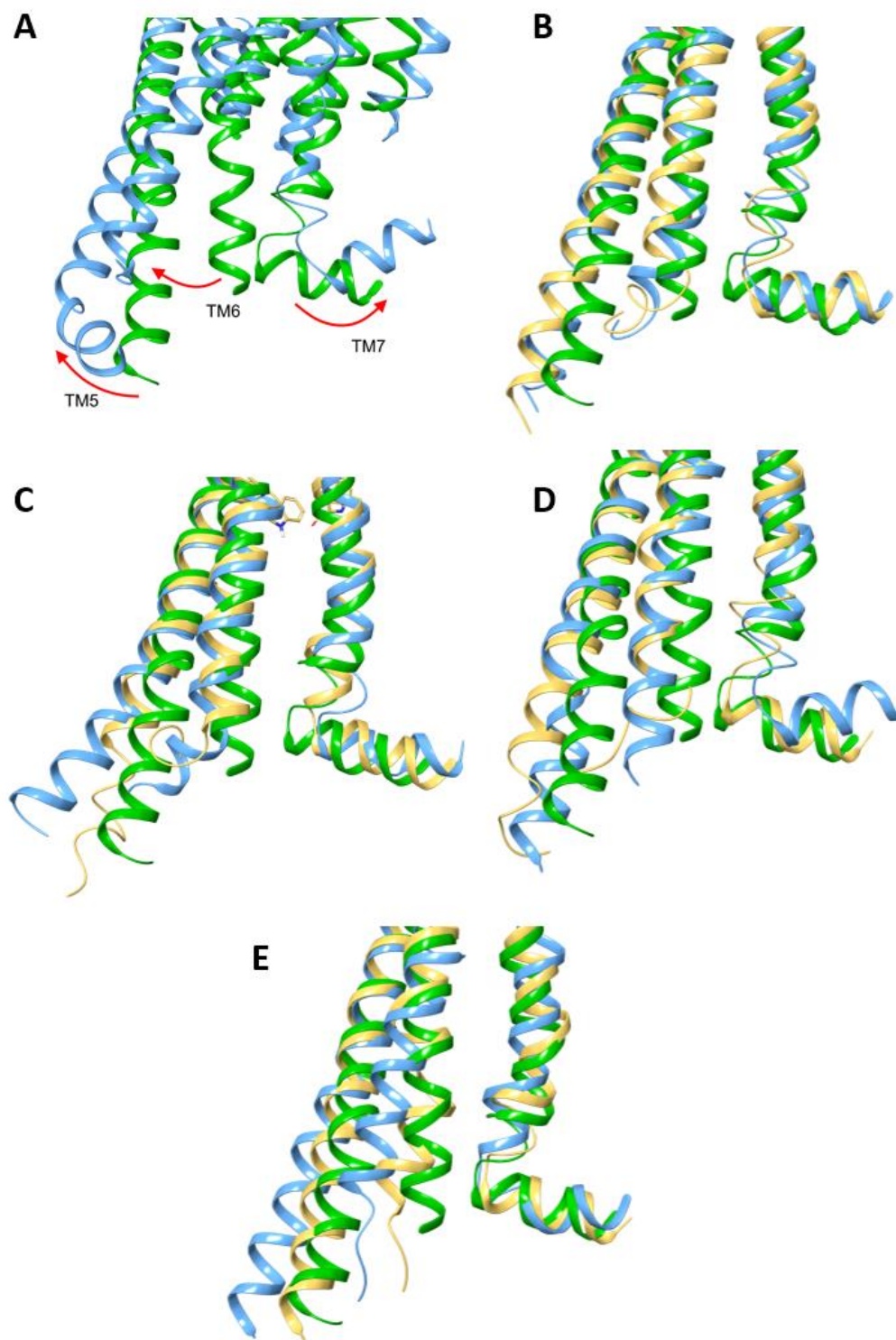


Figure 7. Superimposed structures of CB1 post MD simulation showing helix movement and receptor activation. Receptor with no ligand is represented in green, receptor with the ligand **L-pocket** in blue and receptor with the ligand originating in the **S-pocket** in

orange. (A) **AM11542** (B) **THCV** (C) **THB** (D) **THC** (E) **THCP**.

Taking a closer look at the toggle switches following MD simulations, the reason for the partial loop movement can be observed. The alkyl chain of **AM11542** extends deep into the CB1 pocket, hitting both F200 and W356 toggle switches and significant movement is observed in both (Fig. 8A). In the case of **THCV**, little movement is observed in the toggle residues, with a slight shift in F200 but not enough to trigger activation (Fig. 8B). **THCB** sits deeper in the pocket and as a result in addition to this slight shift in F200, W356 also experience a slight shift downwards. **THC** interacts effectively with F200 and a significant rotation is observed (Fig. 8D). Lastly, **THCP** sits significantly deeper in the pocket and can interact with both toggle residues in a manner like **AM11542** (Fig. 8E). In all cases, the ligands in the **L-pocket** resulted in a more significant movement of toggle residues compared to those in the **S-pocket**.

This indicates that the ability of the ligands to interact with this toggle residues is key to receptor activation and that smaller ligands with shorter chains fail to induce the structural changes required for full activation. Instead, what occurs is a partial activation, characterized by partial movement of TM5, 6, and 7, which correlates to the degree of how well the ligands are able to interact with either F200, W256 or both. This explains why some ligands such as **THC** behave as partial agonists, despite their high binding affinities and provides insight into the mechanism of partial agonists. This also highlights the importance of looking beyond the binding affinity when designing new ligands for receptors. The method through which they enter the binding pocket, in this case through the lipid membrane, is a key factor, along with the exact binding mode and residues that ligand interacts with. Depending on the active site residues that are interacted with, vastly different biological effects can be observed.

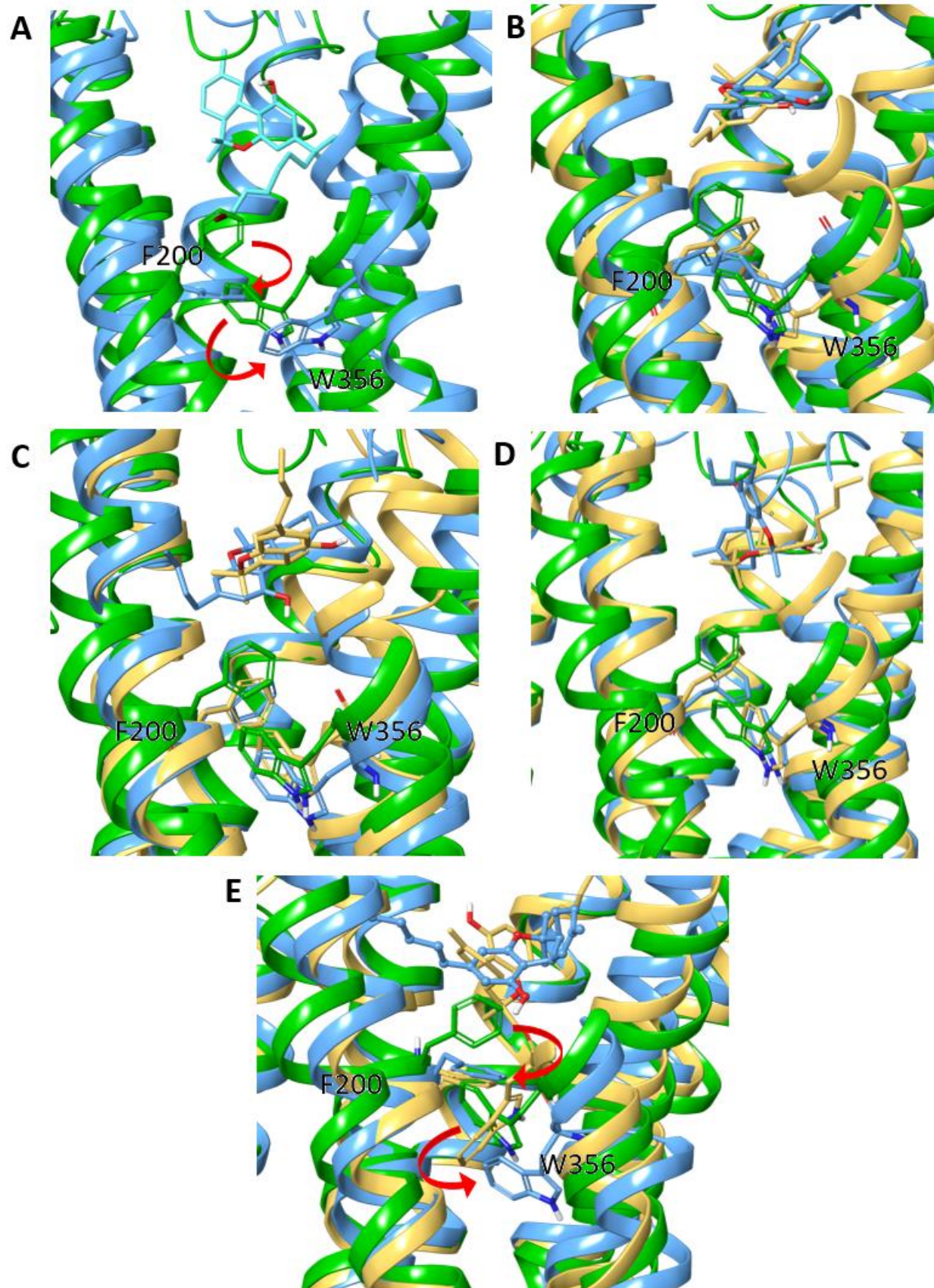


Figure 8. Superimposed structures of CB1 post MD simulation showing positions of toggle switches F200 and W356. Receptor with no ligand is represented in green, receptor with the ligand originating in the **L-pocket** in blue and receptor with the ligand originating in the **S-pocket** in orange. (A) **AM11542** (B) **THCV** (C) **THB** (D) **THC** (E) **THCP**.

CREDIT: Conceptualization: FS and JFT; Funding acquisition JFT; Investigation, FS and DM; Methodology, all authors; Supervision, JFT; Visualization FS; Writing original draft, FS and DM; Writing review and editing, All authors.

Acknowledgments The authors would like to thank Dr. Maryam Kosar for helpful comments on the article. The research was funded by the Natural Sciences and Engineering Research Council of Canada (2018-06338 and 530680-18 to JFT). FS, DM, SM, and JFT would like to highlight that this work was made possible by the facilities of the Shared Hierarchical Academic Research Computing Network (SHARCNET: www.sharcnet.ca) and Compute/Calcul Canada.

Supporting Information: Additional tables of data, figures, computational data, and full co-ordinates for optimized structures discussed, along with videos of the receptor-ligand complex and MD simulation videos are available in the supporting information files.

1. Shahbazi, F.; Grandi, V.; Banerjee, A.; Trant, J. F., Cannabinoids and cannabinoid receptors: The story so far. *iScience* **2020**, *23* (7), 101301.
2. (a) Piscitelli, F.; Ligresti, A.; La Regina, G.; Coluccia, A.; Morera, L.; Allarà, M.; Novellino, E.; Di Marzo, V.; Silvestri, R., Indole-2-carboxamides as allosteric modulators of the cannabinoid CB₁ receptor. *J. Med. Chem.* **2012**, *55* (11), 5627-31; (b) Shao, Z.; Yan, W.; Chapman, K.; Ramesh, K.; Ferrell, A. J.; Yin, J.; Wang, X.; Xu, Q.; Rosenbaum, D. M., Structure of an allosteric modulator bound to the CB₁ cannabinoid receptor. *Nat. Chem. Biol.* **2019**, *15* (12), 1199-1205.
3. Bow, E. W.; Rimoldi, J. M., The structure-function relationships of classical cannabinoids: CB₁/CB₂ modulation. *Perspect. Med. Chem.* **2016**, *8*, 17-39.
4. Citti, C.; Linciano, P.; Russo, F.; Luongo, L.; Iannotta, M.; Maione, S.; Laganà, A.; Capriotti, A. L.; Forni, F.; Vandelli, M. A.; Gigli, G.; Cannazza, G., A novel phytocannabinoid isolated from *Cannabis sativa* L. with an *in vivo* cannabimimetic activity higher than Δ⁹-tetrahydrocannabinol: Δ⁹-Tetrahydrocannabiphorol. *Sci. Rep.* **2019**, *9* (1), 20335.
5. Linciano, P.; Citti, C.; Luongo, L.; Belardo, C.; Maione, S.; Vandelli, M. A.; Forni, F.; Gigli, G.; Laganà, A.; Montone, C. M.; Cannazza, G., Isolation of a high-affinity cannabinoid for the human CB₁ receptor from

a medicinal *Cannabis sativa* variety: Δ^9 -tetrahydrocannabitol, the butyl homologue of Δ^9 -tetrahydrocannabinol. *J. Nat. Prod.* **2020**, *83* (1), 88-98.

6. Jung, S. W.; Cho, A. E.; Yu, W., Exploring the ligand efficacy of cannabinoid receptor 1 (CB1) using molecular dynamics simulations. *Sci. Rep.* **2018**, *8* (1), 13787.

7. Rosenthaler, S.; Pöhn, B.; Kolmanz, C.; Nguyen Huu, C.; Krewenka, C.; Huber, A.; Kranner, B.; Rausch, W.-D.; Moldzio, R., Differences in receptor binding affinity of several phytocannabinoids do not explain their effects on neural cell cultures. *Neurotoxicol. Teratol.* **2014**, *46*, 49-56.

8. McPartland, J. M.; Glass, M.; Pertwee, R. G., Meta-analysis of cannabinoid ligand binding affinity and receptor distribution: Interspecies differences. *Br. J. Pharmacol.* **2007**, *152* (5), 583-93.

9. Iwamura, H.; Suzuki, H.; Ueda, Y.; Kaya, T.; Inaba, T., *In vitro* and *in vivo* pharmacological characterization of JTE-907, a novel selective ligand for cannabinoid CB2 receptor. *J. Pharmacol. Exp. Ther.* **2001**, *296* (2), 420-5.

10. Pagé, D.; Balaux, E.; Boisvert, L.; Liu, Z.; Milburn, C.; Tremblay, M.; Wei, Z.; Woo, S.; Luo, X.; Cheng, Y.-X.; Yang, H.; Srivastava, S.; Zhou, F.; Brown, W.; Tomaszewski, M.; Walpole, C.; Hodzic, L.; St-Onge, S.; Godbout, C.; Salois, D.; Payza, K., Novel benzimidazole derivatives as selective CB₂ agonists. *Bioorg. Med. Chem. Lett.* **2008**, *18* (13), 3695-3700.

11. Pertwee, R. G., The diverse CB1 and CB2 receptor pharmacology of three plant cannabinoids: Δ^9 -tetrahydrocannabinol, cannabidiol and Δ^9 -tetrahydrocannabivarin. *Br. J. Pharmacol.* **2008**, *153* (2), 199-215.

12. Husni, A. S.; McCurdy, C. R.; Radwan, M. M.; Ahmed, S. A.; Slade, D.; Ross, S. A.; ElSohly, M. A.; Cutler, S. J., Evaluation of phytocannabinoids from high potency *Cannabis sativa* using *in vitro* bioassays to determine structure-activity relationships for cannabinoid receptor 1 and cannabinoid receptor 2. *Med. Chem. Res.* **2014**, *23* (9), 4295-4300.

13. Dutta, S.; Selvam, B.; Das, A.; Shukla, D., Mechanistic origin of partial agonism of tetrahydrocannabinol for cannabinoid receptors. *J. Biol. Chem.* **2022**, *298* (4), 101764.

14. McPartland, J. M.; MacDonald, C.; Young, M.; Grant, P. S.; Furkert, D. P.; Glass, M., Affinity and efficacy studies of tetrahydrocannabinolic acid A at cannabinoid receptor types one and two. *Cannabis Cannabinoid Res.* **2017**, *2* (1), 87-95.

15. Halgren, T. A.; Murphy, R. B.; Friesner, R. A.; Beard, H. S.; Frye, L. L.; Pollard, W. T.; Banks, J. L., Glide: A new approach for rapid, accurate docking and scoring. 2. Enrichment factors in database screening. *J. Med. Chem.* **2004**, *47* (7), 1750-9.

16. Lyne, P. D.; Lamb, M. L.; Saeh, J. C., Accurate prediction of the relative potencies of members of a series of kinase inhibitors using molecular docking and MM-GBSA scoring. *J. Med. Chem.* **2006**, *49* (16), 4805-8.

17. Ji, B.; Liu, S.; He, X.; Man, V. H.; Xie, X.-Q.; Wang, J., Prediction of the binding affinities and selectivity for CB1 and CB2 ligands using homology modeling, molecular docking, molecular dynamics simulations, and MM-PBSA binding free energy calculations. *ACS Chem. Neurosci.* **2020**, *11* (8), 1139-1158.

18. Hua, T.; Vemuri, K.; Nikas, S. P.; Laprairie, R. B.; Wu, Y.; Qu, L.; Pu, M.; Korde, A.; Jiang, S.; Ho, J. H.; Han, G. W.; Ding, K.; Li, X.; Liu, H.; Hanson, M. A.; Zhao, S.; Bohn, L. M.; Makriyannis, A.; Stevens, R. C.; Liu, Z. J., Crystal structures of agonist-bound human cannabinoid receptor CB1. *Nature* **2017**, *547* (7664), 468-471.

19. Hua, T.; Li, X.; Wu, L.; Iliopoulos-Tsoutsouvas, C.; Wang, Y.; Wu, M.; Shen, L.; Johnston, C.; Nikas, S.; Song, F.; Song, X.; Yuan, S.; Sun, Q.; Wu, Y.; Jiang, S.; Benchama, O.; Stahl, E.; Zvonok, N.; Zhao, S.; Liu, Z.-J., Activation and signaling mechanism revealed by cannabinoid receptor-G i complex structures. *Cell* **2020**, *180*.

20. (a) Drake, D. J.; Jensen, R. S.; Busch-Petersen, J.; Kawakami, J. K.; Concepcion Fernandez-Garcia, M.; Fan, P.; Makriyannis, A.; Tius, M. A., Classical/nonclassical hybrid cannabinoids: Southern aliphatic chain-functionalized C-6 β methyl, ethyl, and propyl analogues. *J. Med. Chem.* **1998**, *41* (19), 3596-3608;

- (b) Tius, M. A.; Hill, W. A. G.; Zou, X. L.; Busch-Petersen, J.; Kawakami, J. K.; Fernandez-Garcia, M. C.; Drake, D. J.; Abadji, V.; Makriyannis, A., Classical/non-classical cannabinoid hybrids; Stereochemical requirements for the southern hydroxyalkyl chain. *Life Sci.* **1995**, *56* (23), 2007-2012.
21. Showalter, V. M.; Compton, D. R.; Martin, B. R.; Abood, M. E., Evaluation of binding in a transfected cell line expressing a peripheral cannabinoid receptor (CB2): identification of cannabinoid receptor subtype selective ligands. *J. Pharmacol. Exp. Ther.* **1996**, *278* (3), 989-99.
 22. Gareau, Y.; Dufresne, C.; Gallant, M.; Rochette, C.; Sawyer, N.; Slipetz, D. M.; Tremblay, N.; Weech, P. K.; Metters, K. M.; Labelle, M., Structure activity relationships of tetrahydrocannabinol analogues on human cannabinoid receptors. *Bioorg. Med. Chem. Lett.* **1996**, *6* (2), 189-194.
 23. Rhee, M.-H.; Vogel, Z.; Barg, J.; Bayewitch, M.; Levy, R.; Hanuš, L.; Breuer, A.; Mechoulam, R., Cannabinol derivatives: Binding to cannabinoid receptors and inhibition of adenylyl cyclase. *J. Med. Chem.* **1997**, *40* (20), 3228-3233.
 24. Huffman, J. W.; Yu, S.; Showalter, V.; Abood, M. E.; Wiley, J. L.; Compton, D. R.; Martin, B. R.; Bramblett, R. D.; Reggio, P. H., Synthesis and pharmacology of a very potent cannabinoid lacking a phenolic hydroxyl with high affinity for the CB2 receptor. *J. Med. Chem.* **1996**, *39* (20), 3875-7.
 25. Charalambous, A.; Lin, S.; Marciniak, G.; Banijamali, A.; Friend, F. L.; Compton, D. R.; Martin, B. R.; Makriyannis, A., Pharmacological evaluation of halogenated Δ^8 -THC analogs. *Pharmacol. Biochem. Behav.* **1991**, *40* (3), 509-512.
 26. Huffman, J. W.; Miller, J. R. A.; Liddle, J.; Yu, S.; Thomas, B. F.; Wiley, J. L.; Martin, B. R., Structure-activity relationships for 1',1'-dimethylalkyl-Delta8-tetrahydrocannabinols. *Bioorg. Med. Chem.* **2003**, *11* (7), 1397-1410.
 27. Wiley, J. L.; Marusich, J. A.; Huffman, J. W., Moving around the molecule: Relationship between chemical structure and *in vivo* activity of synthetic cannabinoids. *Life Sci.* **2014**, *97* (1), 55-63.
 28. *Induced Fit Docking protocol, Glide, Prime*, Schrödinger, LLC: New York, NY, , 2021.
 29. Sottriffer, C. A., Accounting for induced-fit effects in docking: What is possible and what is not? *Curr. Top. Med. Chem.* **2011**, *11* (2), 179-91.
 30. Zhong, H.; Tran, L. M.; Stang, J. L., Induced-fit docking studies of the active and inactive states of protein tyrosine kinases. *J. Mol. Graphics Modell.* **2009**, *28* (4), 336-346.
 31. (a) Pei, Y.; Mercier, R. W.; Anday, J. K.; Thakur, G. A.; Zvonok, A. M.; Hurst, D.; Reggio, P. H.; Janero, D. R.; Makriyannis, A., Ligand-binding architecture of human CB2 cannabinoid receptor: evidence for receptor subtype-specific binding motif and modeling GPCR activation. *Chem. Biol.* **2008**, *15* (11), 1207-19; (b) Barnett-Norris, J.; Hurst, D. P.; Buehner, K.; Ballesteros, J. A.; Guarnieri, F.; Reggio, P. H., Agonist alkyl tail interaction with cannabinoid CB1 receptor V6.43/I6.46 groove induces a helix 6 active conformation. *Int. J. Quantum Chem.* **2002**, *88* (1), 76-86; (c) Reggio, P. H., Endocannabinoid binding to the cannabinoid receptors: what is known and what remains unknown. *Curr. Med. Chem.* **2010**, *17* (14), 1468-86.
 32. Hurst, D. P.; Grossfield, A.; Lynch, D. L.; Feller, S.; Romo, T. D.; Gawrisch, K.; Pitman, M. C.; Reggio, P. H., A lipid pathway for ligand binding is necessary for a cannabinoid G protein-coupled receptor. *J. Biol. Chem.* **2010**, *285* (23), 17954-64.
 33. (a) Henchoz, Y.; Bard, B.; Guillarme, D.; Carrupt, P.-A.; Veuthey, J.-L.; Martel, S., Analytical tools for the physicochemical profiling of drug candidates to predict absorption/distribution. *Anal. Bioanal. Chem.* **2009**, *394* (3), 707-729; (b) Waring, M. J., Lipophilicity in drug discovery. *Exp. Opin. Drug Discov.* **2010**, *5* (3), 235-248; (c) Pallicer, J.; Rosés, M.; Ràfols, C.; Bosch, E.; Pascual, R.; Port, A., Evaluation of logPo/w values of drugs from some molecular structure calculation software. *ADMET & DMPK* **2014**, *2*.
 34. Mannhold, R.; Poda, G. I.; Ostermann, C.; Tetko, I. V., Calculation of molecular lipophilicity: State-of-the-art and comparison of log P methods on more than 96,000 compounds. *J. Pharm. Sci.* **2009**, *98* (3), 861-893.
 35. *QikProp - 20109- Schrödinger, LLC: New York, NY, 2019.*

36. Pirhadi, S.; Maghooli, K.; Moteghaed, N. Y.; Garshasbi, M.; Mousavirad, S. J., Biomarker Discovery by Imperialist Competitive Algorithm in Mass Spectrometry Data for Ovarian Cancer Prediction. *J Med Signals Sens* **2021**, *11* (2), 108-119.
37. The MathWorks, I., Natick, Massachusetts, United States. *MATLAB and Statistics Toolbox Release* 2012b,.
38. Huffman, J. W.; Liddle, J.; Yu, S.; Aung, M. M.; Abood, M. E.; Wiley, J. L.; Martin, B. R., 3-(1',1'-Dimethylbutyl)-1-deoxy-delta8-THC and related compounds: Synthesis of selective ligands for the CB2 receptor. *Bioorg. Med. Chem.* **1999**, *7* (12), 2905-14.
39. Prandi, C.; Blangetti, M.; Namdar, D.; Koltai, H., Structure-activity relationship of cannabis derived compounds for the treatment of neuronal activity-related diseases. *Molecules* **2018**, *23* (7).
40. Gomez-Jeria, J. S.; Soto-Morales, F.; Rivas, J.; Sotomayor, A., A theoretical structure-affinity relationship study of some cannabinoid derivatives. *J. Chil. Chem. Soc.* **2008**, *53*, 1382-1388.
41. (a) McAllister, S. D.; Hurst, D. P.; Barnett-Norris, J.; Lynch, D.; Reggio, P. H.; Abood, M. E., Structural mimicry in class A G protein-coupled receptor rotamer toggle switches: The importance of the F3.36(201)/W6.48(357) interaction in cannabinoid CB1 receptor activation. *J. Biol. Chem.* **2004**, *279* (46), 48024-37; (b) Latek, D.; Kolinski, M.; Ghoshdastider, U.; Debinski, A.; Bombolewski, R.; Plazinska, A.; Jozwiak, K.; Filipek, S., Modeling of ligand binding to G protein coupled receptors: cannabinoid CB1, CB2 and adrenergic beta 2 AR. *J. Mol. Model.* **2011**, *17* (9), 2353-66.
42. Shao, Z.; Yin, J.; Chapman, K.; Grzemska, M.; Clark, L.; Wang, J.; Rosenbaum, D. M., High-resolution crystal structure of the human CB1 cannabinoid receptor. *Nature* **2016**, *540* (7634), 602+.
43. Krishna Kumar, K.; Shalev-Benami, M.; Robertson, M. J.; Hu, H.; Banister, S. D.; Hollingsworth, S. A.; Latorraca, N. R.; Kato, H. E.; Hilger, D.; Maeda, S.; Weis, W. I.; Farrens, D. L.; Dror, R. O.; Malhotra, S. V.; Kobilka, B. K.; Skiniotis, G., Structure of a signaling cannabinoid receptor 1-G protein complex. *Cell* **2019**, *176* (3), 448-458.e12.